

Wind Turbine Blade Design

Calvin Phelps, John Singleton

Cornell University, Sibley School of Engineering

Advisors: Rajesh Bhaskaran, Alan T. Zehnder

The overall goal of our project was to gain an understanding of wind turbine blades sufficient to develop Figures of Merit analyzing the tradeoffs between structure, material, cost, and other qualities in order to optimize the design of a large wind turbine blade. Due to the size of emergent utility-scale wind turbines, concerns that in current technology are minimal (such as weight), have the potential to add new dimensions to the driving design conditions. These additions are not necessarily captured by traditional wind turbine analytical solutions, and we wished to factor them into our analyses.

As our ultimate goal was to iterate our design based on the aforementioned figures of merit, it was necessary to develop a means of quickly developing and evaluating various blade geometries and construction methodologies. To that end, we modeled and evaluated our blade design using ANSYS, a finite element program that, when used properly, allowed us to quickly evaluate designs under a variety of loading conditions and material constraints.

Over the course of this year we were able to develop analytical solutions to various aerodynamic loads, along with rudimentary root size estimations. We used these analytic solutions to guide our initial blade sizing and geometry, but transitioned to computational analysis tools like WT_Perf and ANSYS later on in order to more efficiently vary key design parameters and obtain additional accuracy in load profiles. We were ultimately able to optimize across several key design constraints for the blade, and compared our computational results with our initial analytic estimations to mixed results. While we were able to optimize our blade design at key core levels, we were ultimately unable to develop in detail many of the desired figures of merit. We obtained FOM for structural stability and cost, but future work will be required to further evaluate these and others.

Initial Analytical Results

In the first half of the year we focused our efforts on obtaining closed form solutions for various blade loads and structural requirements. These results were difficult to iterate, and were thus not conducive to the optimization we desired to perform, but nonetheless provided a useful first pass at designing our turbine blade. We will briefly reiterate some of the key findings from this work.

The turbine blade design is guided perhaps most strongly by the flapwise bending moments. From (Manwell, McGowan, & Rogers, 2002), this moment is defined by

$$M_{\beta} = \frac{2}{3} \frac{T}{B} R \quad (1)$$

where T is thrust, B the number of blades, and R the radius of the turbine blade. The thrust coefficient (and from it, thrust) is a function of the axial induction factor a, and is defined by

$$C_T = 4a(1 - a) \quad (2)$$

For the purposes of our analyses, we assumed the Betz limit of 1/3 for our axial induction factor. This represents a very conservative assumption, and accordingly drives up our expected moments beyond what would typically be expected for a blade of this size and type. Using these parameters and the relation between thrust and its coefficient, we determined the following for our blade:

Table 1: Aerodynamic Loads and Load Coefficients

	Rated Wind Speed (12 m/s)	Cut-out Speed (20 m/s)
a	.333	.333
C_T	.889	.889
T	436 kN	1210 kN
M_β	4.072 MN-m	11.31 MN-m
V	145 kN	404 kN

Additionally, we also sought to obtain the edgewise moment upon our blade. This moment is defined by the equation

$$M_E = \frac{Torque}{B} + W \frac{R}{3} \quad (3)$$

where M_E is the edgewise bending moment, and W the weight of the blade. Torque is simply the power of the turbine (1.5 MW) over the angular velocity (1.15 rad/s minimum, 1.76 rad/s maximum) of the blade. The moment arm here was assumed to be 1/3 the full blade length, in the belief that for a turbine blade with taper it is likely the center of mass lies between the blade root and midpoint. We also calculated the centrifugal force induced on the blade by its axial rotation. Where m is the mass of the blade, the relation is simply

$$F_c = mR\Omega \quad (4)$$

The mass of the blade in this first pass calculation was assumed to be 10 metric tons. The results from our findings can be seen in Table (2).

Table 2: Additional Aerodynamic Loads

	Low Rotational Velocity (1.15 rad/s)	High Rotational Velocity (20 m/s)
Torque	1.3 MN-m	.853 MN-m
M_E	1.81 MN-m	1.66 MN-m
F_c	484 kN	739 kN

Accordingly, we determined that the flapwise moment was indeed the key driver of our blade design, as the edgewise and centrifugal force terms are small in comparison. Using a blade design study from Sandia National Laboratory (TPI Composites, Inc., 2002), we were also able to determine the extreme loads for our blade when parked in 70 m/s winds. This calculation yielded a bending moment of 10.54 MN-m, a high value to be sure, but still lower than our very conservatively estimated flapwise bending moment.

An additional key design parameter that we determined was the necessary root thickness for our blade given the above load conditions. This thickness will be defined from our material properties, which can be seen below.

Table 3: Properties of Multidirectional QQ1 E-Glass Laminate (Samborsky, Wilson, & Mandell, 2007)

Property	Value (MPa)
Young's Modulus	33000
Tensile Strength	869
Compressive Strength	690

Generally speaking, the maximum stress of a body is related to the bending moment by the equation

$$\sigma_{\max} = \frac{M_{\beta} h}{I_{\beta}} \quad (5)$$

where I_{β} is the moment of inertia, and h the distance from the chordline, a quantity we will refer to as height. σ_{\max} is the material maximum stress, which for QQ1 E-glass in compression (and incorporating a safety factor of 2) is 345 MPa. For a hollow circular root section, the moment of inertia I_{β} is defined as

$$I_{\beta} = \frac{1}{4} \pi (R_o^4 - R_i^4) \quad (6)$$

Accordingly, the thickness t of the blade can be calculated using the equation

$$t = R_o - \left(R_o^4 - \frac{4M_{\beta} h}{\pi \sigma_{\max}} \right)^{1/4} \quad (7)$$

We were able to therefore calculate the necessary thickness for our blade root solely from the geometry and general performance characteristics of the blade. The resultant thicknesses from this analysis are given by Table (4).

Table 4: Necessary Blade Root Thickness at Rated and Cut-out Speeds

	Thickness (mm)
Rated Wind Speed (12 m/s)	3.78
Cut-out Speed (20 m/s)	10.6

These values represent our first pass at determining necessary blade geometry, and did not include such concerns as fatigue, additional materials, or internal components. Going forward, we will look at the effects such concerns have on these values.

Incorporation of Fatigue into Design Parameters

A given material’s strength can decrease substantially over the course of its lifetime. Repeated loading and unloading of the material causes progressive and localized structural damage, and the resultant damage will lower the ultimate stress the material is able to endure without failure. This process of progressive material weakening is known as fatigue, and becomes an important design parameter when a material experiences many load cycles within its lifetime.

For a wind turbine, the expected life of a given blade may be estimated around 20 years. For this length of time, one can expect the blade to experience around 60 million load cycles. Examining the S-n curve for our blade material, it is possible to infer the ultimate limits of our blade for a 20 year lifetime. This fatigue limit can serve as an additional limiting factor for the analysis of our blade design.

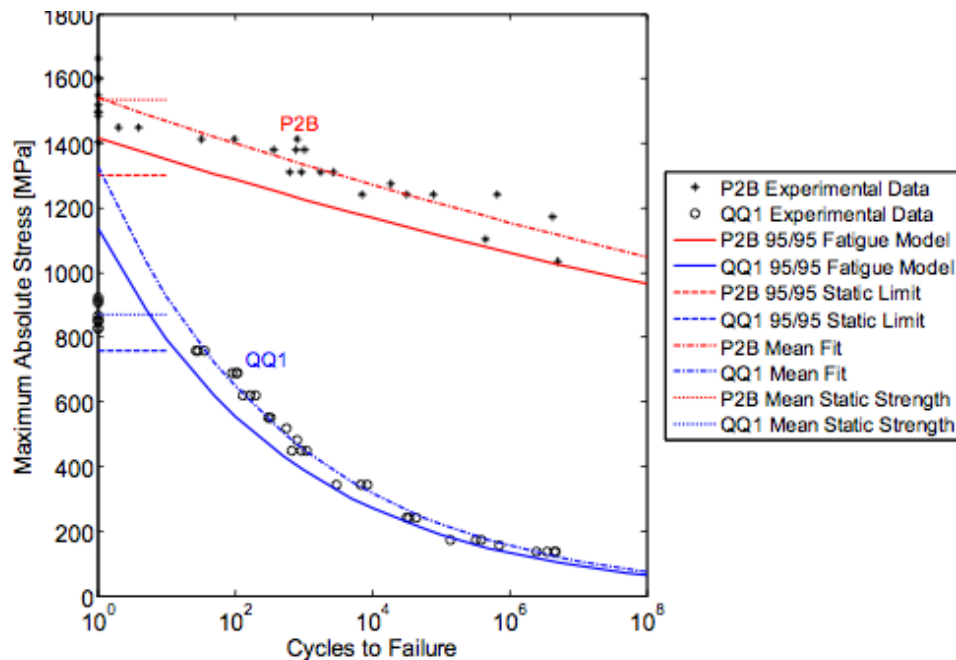


Figure 1: S-n Curve for QQ1 E-Glass and P2B Carbon/E-Glass Laminate (Samborsky, Wilson & Mandell, 2007)

As our blade is not a single material, we must look at how both the QQ1 E-glass and carbon laminate respond to fatigue limits. Using Figure (1), we are able to determine the following fatigued material limits for our blade.

Table 5: Fatigue Limits for Turbine Materials

	Maximum Allowable Stress at 60e6 cycles (MPa)
QQ1-E-glass	120
P2B Carbon Laminate	1200

As is expected, the ultimate stress of the fatigued carbon fiber is considerably higher than the allowable stress for the E-glass. Accordingly, the stress limit of the blade is determined by the strength of the E-glass used in the skin of the blade. As this fatigue limit occurs at the end of the expected lifespan of the turbine blade anyway, there is no need to incorporate an additional safety factor on this value, and we may assume the maximum allowable stress in our turbine blade to be 120 MPa.

It is worth noting that this stress value is below the one computed by our first pass analytic solution, so the necessary skin thickness of our blade is now higher than what was computed then. Updated thickness values for the first pass analytics are included in the table below.

Table 6: Necessary Blade Root Thickness at Rated and Cut-out Speeds (Incorporating Fatigue)

	Thickness (mm)
Rated Wind Speed (12 m/s)	11.0
Cut-out Speed (20 m/s)	31.5

WT_Perf Methodology/Data

In order to determine the shape of the blade, we utilized a program developed by the National Wind Technology Center called WT_Perf. WT_Perf uses blade element momentum theory in order to approximate blade loading as well as the power output. The objective of the work with WT_Perf was to find a twist, chord, and airfoil configuration for a 41.25 m blade that produces 1.5MW in a wind speed of 10 m/s. The length, power output and wind speed come from the technical specifications of the GE 1.5 XLE wind turbine. The wind speed of 10 m/s is half the cut-out speed for the 1.5 XLE.

We used test file “Test04_WP15.wtp” as the starting point for our WT_Perf calculations. The test file uses 19 blade elements and three airfoils: S818, S825 and S826. It also uses the non-dimensional version of blade element momentum theory, which allowed us to easily scale our results to the specifications of the 1.5 XLE. Non-dimensional chord lengths and airfoil distributions were not changed, but we did have to iterate twist to achieve the desired power output. The optimal twist arrangement was found essentially by guess and check iteration. The table below displays the final geometry arrangement that was chosen.

Table 7: WT_Perf Blade Geometry

Element	r/R	Twist °	C/R	Airfoil
1	0.075	42	0.0614	S818
2	0.125	32	0.06826	
3	0.175	23	0.07452	
4	0.225	15	0.07782	
5	0.275	11.5	0.07543	
6	0.325	8.2	0.07188	
7	0.375	7	0.06832	
8	0.425	6	0.06479	
9	0.475	5	0.06126	
10	0.525	4	0.05771	S825
11	0.575	4.15	0.05415	
12	0.625	3.85	0.05062	
13	0.675	3.25	0.04707	
14	0.725	2.75	0.0436	
15	0.775	1.25	0.04024	
16	0.825	0.75	0.03704	
17	0.875	0.55	0.03385	S826
18	0.925	0.85	0.03066	
19	0.975	0.05	0.02747	

The second column in the table above is the non-dimensional blade element position and the fourth column is the non-dimensional chord length. The table below displays the power output of a three blade wind turbine with the aforementioned geometry arrangement for rated wind speed (10 m/s) and cut-out wind speed (20 m/s) for various pitch angles.

Table 8: WT_Perf Power Output for Given Blade Geometry

Pitch (deg)	Power [kW] with 10 m/s wind	Power [kW] with 20 m/s wind
-4	1502.381	1541.013
-3	1550.928	2010.38
-2	1596.825	2488.243
-1	1623.915	2961.509
0	1627.014	3413.535
1	1611.397	3834.488
2	1580.034	4227.44
3	1535.555	4581.086
4	1480.177	4863.556

Additionally, we sought to determine the flapwise moment given by Wt_Perf, as this should be a more accurate calculation than that given by equation (1) from (Manwell, McGowan, & Rogers, 2002). The flapwise moments for our turbine are given below for rated, cut-out, and extreme wind speeds.

Table 9: Flapwise Moments from WT_Perf

	Rated Wind Speed 10 m/s	Cut-out Wind Speed 20 m/s	Extreme Winds 70 m/s wind
Pitch (deg)	0	0	82
M_{β} (kN-m)	2212	2875	96.7

The flapwise moments generated can thus be seen to be smaller than those calculated by equation (1). This is to be expected, however, as those moment values were calculated assuming an axial induction factor of 1/3. This represents the most conservative estimate possible to generate a given amount of power, and drives up the thrust quantity (and from that, M_{β}) considerably. Notably, the moment generated by extreme winds can be driven down significantly by pitching the blades appropriately into the wind. Were the blade to have no pitch (0 degrees), the moment in extreme winds would be 7386 kN-m. So long as we are able to pitch our blade, however, it is possible to keep even extreme winds from damaging the turbine blade.

Transformation of WT_Perf Loads

The loads given by WT_Perf are incredibly useful in providing a comprehensive numerical analysis of the edge and flapwise forces at a variety of operating conditions, allowing for an analysis of blade element loads given different blade pitch, wind speed, and more. These loads are all given in the local coordinates of the airfoil, however, and are thus not useful in applying appropriate load conditions within ANSYS, which operates by default in a global coordinate system.

The loads given by WT_Perf must therefore be transformed into their equivalent forces in the global coordinate system. In order to understand this transformation, it is probably best to define the system as follows:

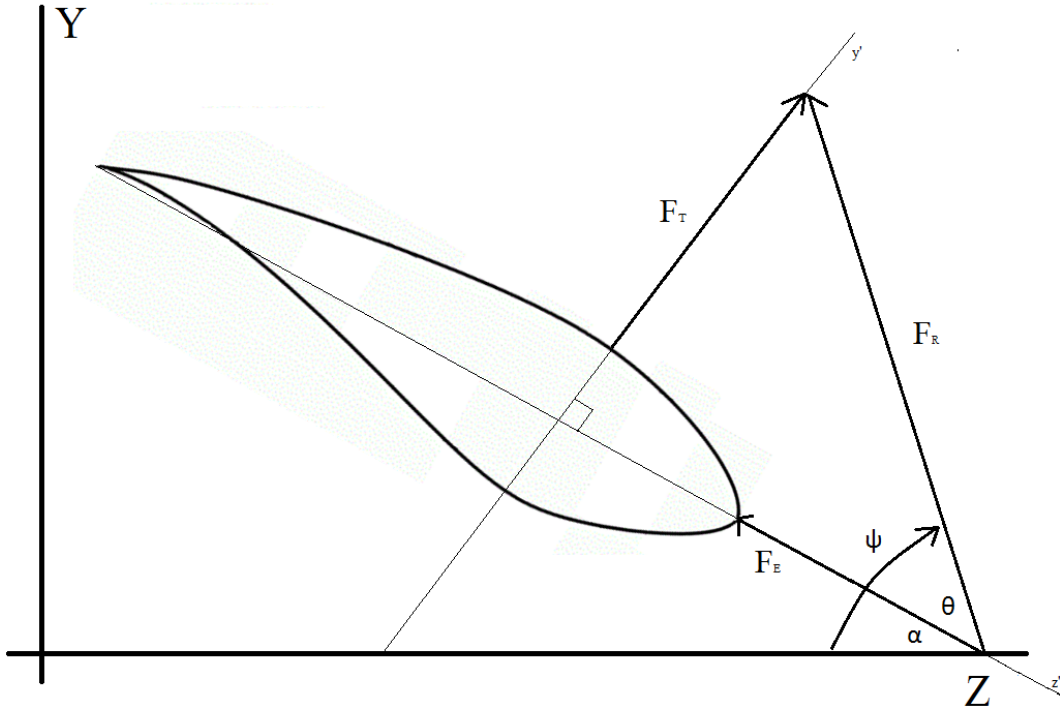


Figure 2: Airfoil Aero Forces and Relevant Transformation Geometries (not to scale)

As seen above, the thrust and edge forces are orthogonal, meaning the resultant force in the local coordinate system can be computed using Pythagoras' Theorem, or

$$F_R = \sqrt{F_T^2 + F_E^2} \quad (8)$$

This resultant force is oriented at some angle within the local coordinate system, and is defined by the length of its component sides, F_T and F_E . This angle is given by

$$\theta = \tan^{-1}\left(\frac{F_T}{F_E}\right) \quad (9)$$

θ is the resultant force angle in the local coordinate system, but the local coordinates are themselves offset by some angle α , or the twist for that airfoil section. This twist angle is known from our WT_Perf data, as it is the twist angle given for that airfoil element. The angle ψ as seen in Figure (2) is the angle that defines the orientation of F_R in the global coordinate system, and is simply θ plus α . The resultant force acting in the global coordinate system has components F_Y and F_Z , which are defined by the equations

$$F_Z = F_R \cos(\psi) \quad (10)$$

$$F_Y = F_R \sin(\psi) \quad (11)$$

Equations (10) and (11) give the forces in the edgewise and flapwise directions in a form that can be input directly into ANSYS. While this process could be done for all sections for which we have WT_Perf data, for simplicity's sake we split the WT_Perf-given loads into five sections. This allowed us to differentiate in a broad sense the load differences across the span of the blade while still allowing for ease of implementation as we iterated blade properties and loading

conditions. It is important to note that the blade twist, just like the blade loads, vary across each section of the blade. To incorporate this shift, we simply used the average twist for the blade for each of the five sections. This aggregation, along with the calculation of F_{z_a} and F_y for the entire blade, can be seen in Tables (10) and (11) for both the rated and cut-out wind cases.

Table 10: Transformation of WT_Perf Loads into Global Coordinate System - Cut-out Case

Relm (% span)	Twist (deg)	Avg Twist (deg)	Thrust (N)	Edge Force (N)	Resultant Force (local coord) (N)	θ (local resultant angle) (deg)	ψ (Global resultant ang)	F_z in Global Coord	F_y in Global Coord
0.075	42	28	5020.	3060	5879.	58.6	86.6	345.2	5868.7
0.125	32								
0.175	23								
0.225	15								
0.275	11.5	8.18	14549.	2543.	14770.	80.1	88.3	447.9	14763.
0.325	8.2								
0.375	7								
0.425	6								
0.475	5	4.25	23172.	4558.	23616.	78.9	83.1	2828.	23446.
0.525	4								
0.575	4.15								
0.625	3.85								
0.675	3.25	2	33637.	8363.	34661.	76.0	78.0	7184.	33909.
0.725	2.75								
0.775	1.25								
0.825	0.75								
0.875	0.55	0.483	39246.	9123.	40292.	76.9	77.4	8792.	39321.
0.925	0.85								
0.975	0.05								
1									

Table 11: Transformation of WT_Perf Loads into Global Coordinate System - Rated Wind Speed Case

Relm (% span)	Twist (deg)	Avg Twist (deg)	Thrust (N)	Edge Force (N)	Resultant Force (local coord) (N)	θ (local resultant angle) (deg)	ψ (Global resultant ang)	F_z in Global Coord	F_y in Global Coord
0.075	42	28	4142.	2697.	4943.	56.9	84.9	436.6	4923.
0.125	32								
0.175	23								
0.225	15								
0.275	11.5	8.18	13340.	3649.	13830.	74.7	82.9	1715.	13723.
0.325	8.2								
0.375	7								
0.425	6								

0.475	5	4.25	22516.	3660.	22811.	80.8	85.0	1981.	22725.
0.525	4								
0.575	4.15								
0.625	3.85								
0.675	3.25	2	30218.	3574.	30428.	83.3	85.3	2517.	30324.
0.725	2.75								
0.775	1.25								
0.825	0.75								
0.875	0.55	0.483	24506.	1974.	24585.	85.4	85.9	1767.	24522.
0.925	0.85								
0.975	0.05								
1	0								

Modeling the Turbine Blade

The analysis of the blade in an analytical fashion yields useful first-pass results about stresses and moments, which is useful in determining basic strength and material requirements. This type of analytical analysis, though useful, is insufficient to properly evaluate the full wind turbine blade.

Accordingly, we sought to use finite element analysis to more accurately capture the loads and stresses generated on the blade geometry by particular loading scenarios. This computational method allows for much greater flexibility in testing out various loads and blade geometries, allowing for an iterative approach to developing our turbine blade.

First, we began by selecting our airfoils. We decided to use the NREL S-series of airfoil as described in (Malcolm and Hansen 2006). These airfoils are in general somewhat thicker than the types typically seen on airplanes due to structural concerns, and are largely insensitive to roughness. As such, they are well suited for turbine blades.

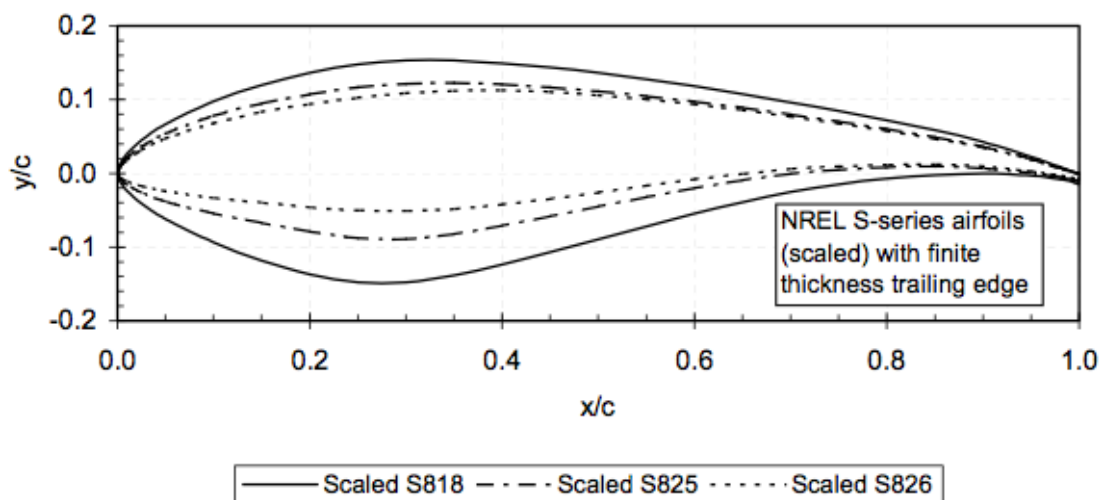


Figure 3: Turbine Blade Airfoils (S818, S825, S826)

The beginning of the blade is the circular hub section. This circular root transitions into the S818 airfoil, which then transitions to the S825 airfoil, which then transitions into the S826 airfoil used at the tip. The full blade geometry, including twist, span, and chord lengths, were determined through WT_Perf analysis and can be seen below.

Table 12: Turbine Blade Geometry

Relm (% span)	Span (m)	Twist (deg)	Chord (% span)	Chord (m)	Airfoil
0.075	3.09375	42	0.06140	2.5328	S818
0.125	5.15625	32	0.06826	2.8157	
0.175	7.21875	23	0.07452	3.0740	
0.225	9.28125	15	0.07782	3.2101	
0.275	11.34375	11.5	0.07543	3.1115	
0.325	13.40625	8.2	0.07188	2.9651	
0.375	15.46875	7	0.06832	2.8182	
0.425	17.53125	6	0.06479	2.6726	
0.475	19.59375	5	0.06126	2.5270	S825
0.525	21.65625	4	0.05771	2.3805	
0.575	23.71875	4.15	0.05415	2.2337	
0.625	25.78125	3.85	0.05062	2.0881	
0.675	27.84375	3.25	0.04707	1.9416	
0.725	29.90625	2.75	0.04360	1.7985	
0.775	31.96875	1.25	0.04024	1.6599	
0.825	34.03125	0.75	0.03704	1.5279	
0.875	36.09375	0.55	0.03385	1.3963	S826
0.925	38.15625	0.85	0.03066	1.2647	
0.975	40.21875	0.05	0.02747	1.1331	
1	41.25	0	0.02424	1	

With the full blade geometry defined, we began the process of building the blade for our FEA model. While it is possible to model and analyze a full wing using just ANSYS, we decided to model the blade using the SolidWorks CAD package instead due to familiarity with that program. As it is possible to import geometry directly from SolidWorks into ANSYS, this seemed to be the most efficient way to manage the creation of the blade.

In order to ensure maximum flexibility and computational efficiency within ANSYS, we designed the blade within SolidWorks as a lofted surface, which is analogous to building with ANSYS' shell elements. Blade design is essentially accomplished by pasting each airfoil element on a plane placed the appropriate distance from the turbine hub (the span distance seen in Table (12)). Then, using the surface loft command, it is possible to connect these various sketches into a single body, letting SolidWorks automatically generate the intermediate blade shape between each defined airfoil. To minimize unnecessary complications in the geometry, we lofted each section using the airfoil leading edge as the loft guide point.

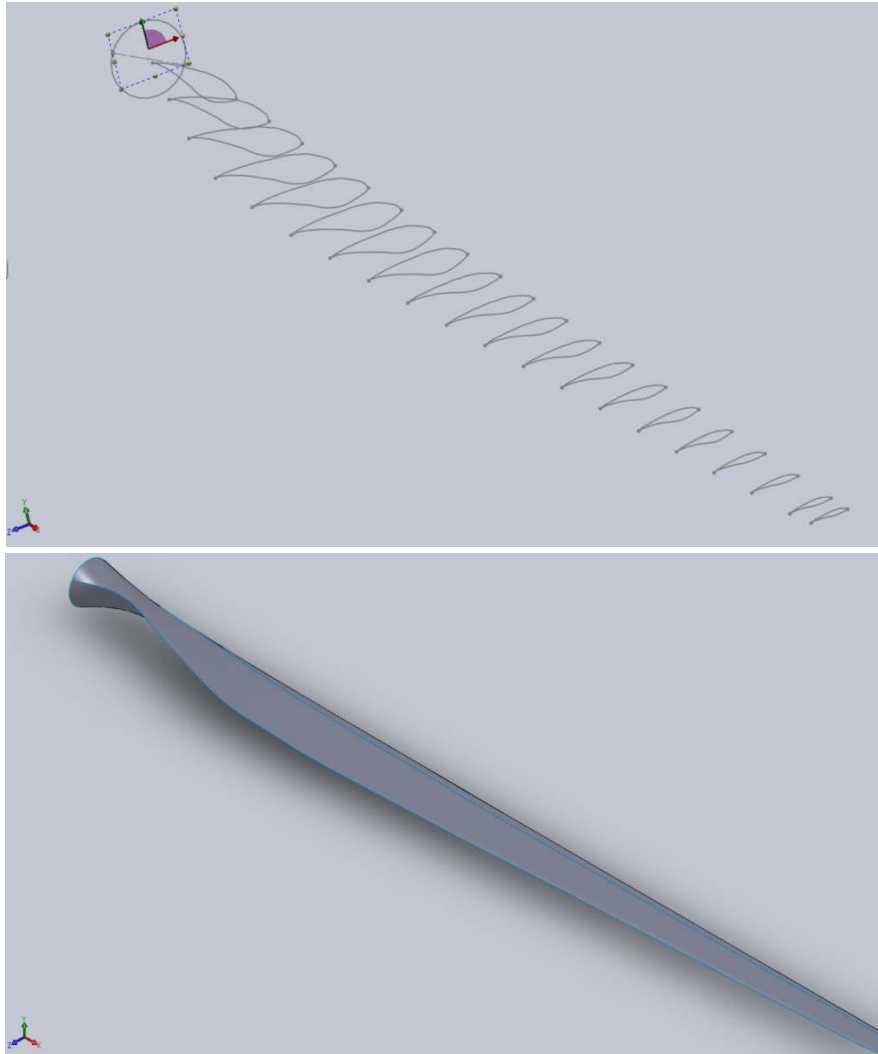


Figure 4: Full Blade Skeleton and Blade as a Lofted Surface

Each airfoil section was created using point data that defines that particular airfoil. This data was obtained by using a program to translate the graphical rendition of the airfoil into (x,y) point data. It is important to note that this data by itself is insufficient to generate a quality blade model, however. The program used is somewhat imprecise, and induces errors (dips and rises) in the airfoil shape if transferred directly into SolidWorks.



Figure 5: S826 Airfoil with Unmodified (top) and Modified (bottom) Point Data

Using SolidWorks' preview tool when importing point data, we were able to modify the point data enough to smooth out the most egregious of these shape errors, While some shape irregularities remained, we assumed the effects of these imperfections to our ANSYS analyses to be negligible. Additionally, it is important to note that the airfoil data had to be separated into the top and bottom sections for each airfoil. In our original attempt to create the blade we brought in each airfoil in its entirety and lofted the blade from these full airfoils, but we found this method yielded problems within ANSYS. The FEA package was not able to properly recognize defining features like the leading and trailing edges, which led to exceedingly complicated meshes or geometries that would not mesh at all, depending on the section analyzed. By separating the SolidWorks lofts into the top and bottom sections we essentially "created" these defining features, ensuring that ANSYS recognized the geometric constraints of the blade and yielded much simpler and efficient meshes.

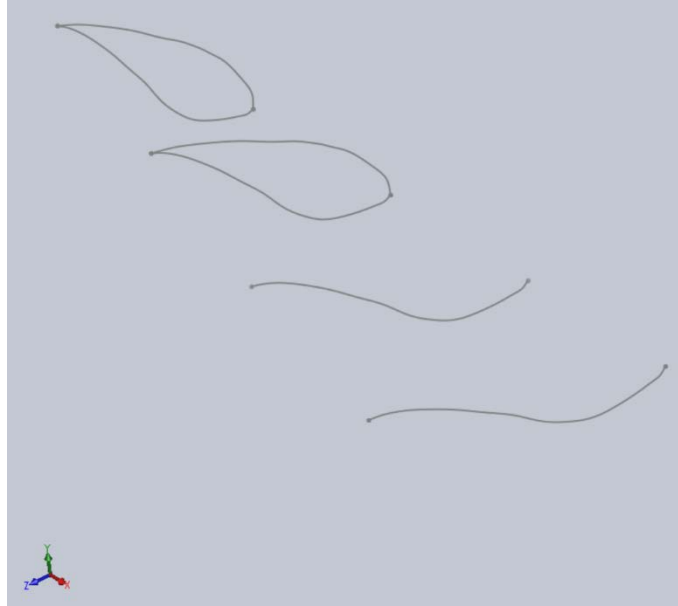


Figure 6: Airfoils - Combined and Bottom Shapes

When designing the blade, one of the key features that governs performance is the twist of each airfoil. The root of the blade is, in general, highly twisted in comparison to the tip. In order to capture this twist, after sketching each airfoil we rotated it by the amount appropriate for that section of the blade. For ease in design, the airfoils were rotated about the leading edge.

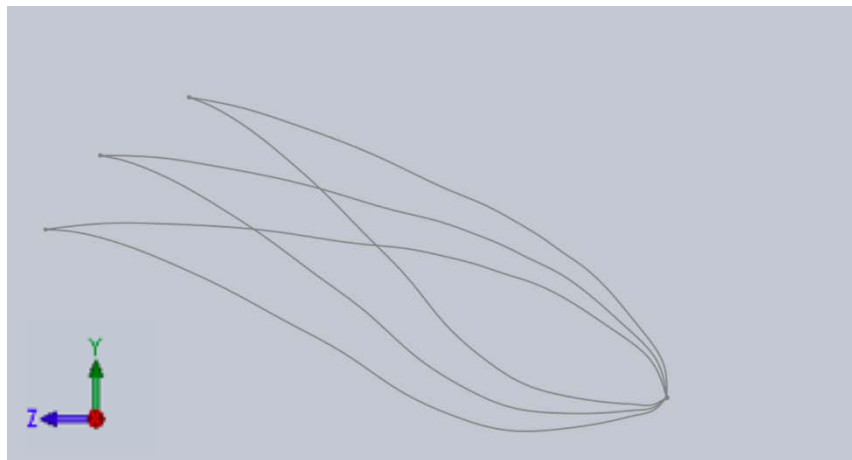


Figure 7: Several Airfoils Rotated About their Leading Edges

With the reference airfoils created, it then became possible to perform a surface loft for the entire blade. Again, it is important to note that this resulted in two distinct lofts within SolidWorks, one loft that runs the length of the blade is the top half of all airfoils, while the second loft was created from the sketches of the bottom halves of the reference airfoils. This distinction includes the circular root of the blade. The root transitions from a circle to an airfoil twisted at 42° , which generates a somewhat complex intermediate geometry. Without the separation of the circle into a distinct top and bottom half, ANSYS was not capable of generating a solution for that section.

With the general shape of the airfoil created, we then turned to the creation and implementation of the blade spar. An airfoil itself, simply by virtue of its geometry, is not capable of effectively supporting transverse loads that induce bending. The blade is made capable of supporting these loads by the inclusion of a spar that runs the length of the blade (beginning at the first reference airfoil). In practice, many wind turbines actually incorporate two spars, placed (very roughly estimated) at 33% and 67% of chord. For the purposes of our analysis, however, we simply incorporated a spar at the quarter chord of the blade. This was accomplished within SolidWorks by creating a new set of sketches to define the spar. Each spar was drawn on the same plane as a reference airfoil, and was placed at the quarter chord and orthogonal to the chord line of that section. Though not technically a part of the airfoil sketch, it was important to build the spar line such that it was defined by the geometry of the airfoil. These relations (SolidWorks building term) allowed the spar to easily be placed at any distance from the leading edge while ensuring that it remained the appropriate height and orientation with respect to the chord line.

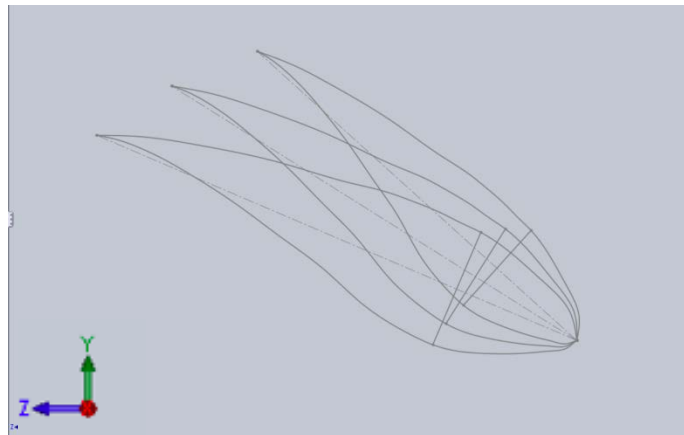


Figure 8: Reference Airfoils with Spar Line

With the creation of the spar lines, we were then able to build the third and final component of the blade by creating a surface loft of the spar lines. To achieve the proper loft (with no unnecessary twists or rotations) we used the tops of the spar lines as the guide points along the length of the blade.. With the creation of the spar, we were finished with the preliminary blade design, and were able to import this geometry into ANSYS for more comprehensive analysis.

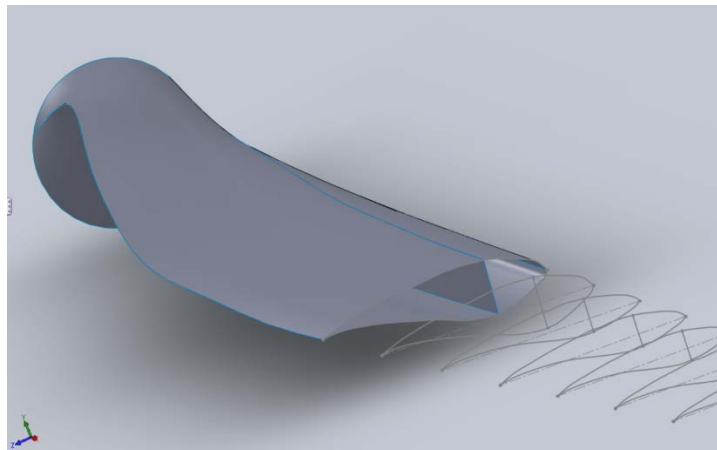


Figure 9: Cross Section of Blade, with Spar and Reference Airfoils Visible

ANSYS Analysis

Varying Thickness Verification

As a part of the blade analysis, it was desirable to incorporate thickness as a function that varies along the length of the blade. There is no method, however, of incorporating varying thicknesses for shell elements within the ANSYS GUI. As a result, custom commands had to be interjected within the simulation in order to specify the varying thicknesses. To test if the thickness commands were working properly, we compared ANSYS results to theoretical results for the following setup.

The geometry consisted of a cantilevered beam with a length of 10 m, a width of 0.5 m and a linearly varying thickness. The root thickness was set to 0.5 m and the thickness at the end was set to 0.1 m. Next, the thicker face (face with 0.5 m x 0.5 m dimensions) was fixed while the thin face (face with 0.5 m x 0.1 m dimensions) was given a transverse load of 100,000N. This setup is illustrated below.

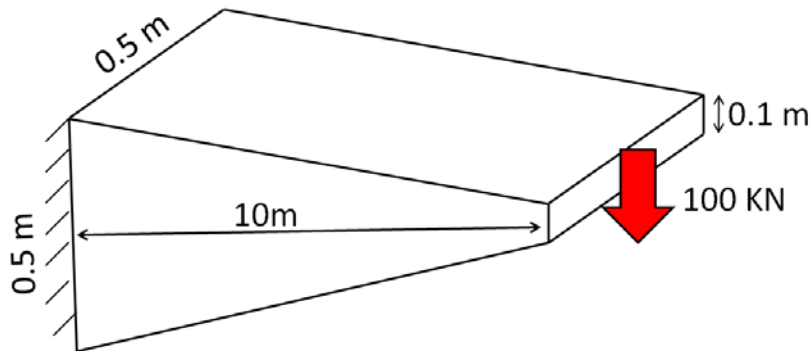


Figure 10: Cantilever Beam with Varying Thickness

The default ANSYS material properties were left unchanged. Thus, the Young's Modulus was that of structural steel, 200 GPa. ANSYS outputted 0.0918 as the tip deflection. Note that since thicknesses are assigned through "Snippet" commands, they do not appear in the images that ANSYS creates.

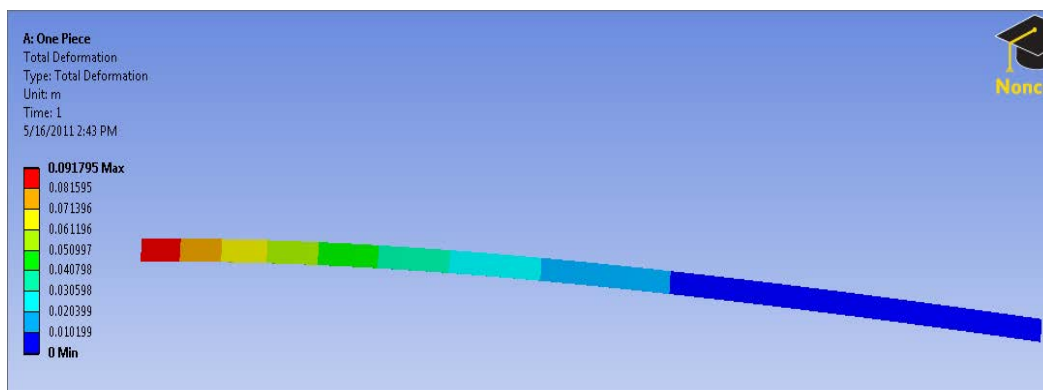


Figure 11: Deflection of Cantilevered Beam

In order to verify these results the second derivative method was used. The following equation was accordingly integrated twice:

$$U'' = \frac{M}{EI} \quad (12)$$

where U is the deflection, M is the moment, E is the Young's Modulus and I the area moment of inertia. The following two boundary conditions were applied during the integration process: $U'(0) = 0$; and $U(0) = 0$. These implement a zero angle and zero displacement constraint, respectively, at the fixed side. The moment of inertia is defined by

$$M = PL \left(1 - \frac{x}{L}\right) \quad (13)$$

where P is the magnitude of the transverse load. The area moment of inertia is defined by the following equation:

$$I_y = \frac{hb^3}{12} \quad (14)$$

It is important to note, however, that thickness h is a function of position. The thickness h is defined by the function $h = 0.5 - 0.04x$.

In order to deal with the complicated integration due to the varying thickness, symbolic integration was used in MATLAB in order to solve for the theoretical tip displacement. The theoretical calculations yielded a tip deflection of 0.0918m. The comparison of FEA and theoretical results are summarized in Table (13).

Table 13: Varying Thickness Cantilever Beam Verification

	Tip Deflection
ANSYS	0.091795 m
Theoretical	0.0918 m

Accordingly, we concluded that thickness commands had been properly implemented and were functioning correctly.

Straight Blade Verification

As part of the verification process, ANSYS results were compared to theoretical results for a straight, constant thickness wing with no spar. The geometry consisted of an S818 airfoil extruded to a length of 10 m, with a thickness of 0.030 m. The geometry was then fixed at one end and assigned a load of 1kN at the opposite end. The load was assigned in the direction perpendicular to the chord. This setup is shown in the following picture.

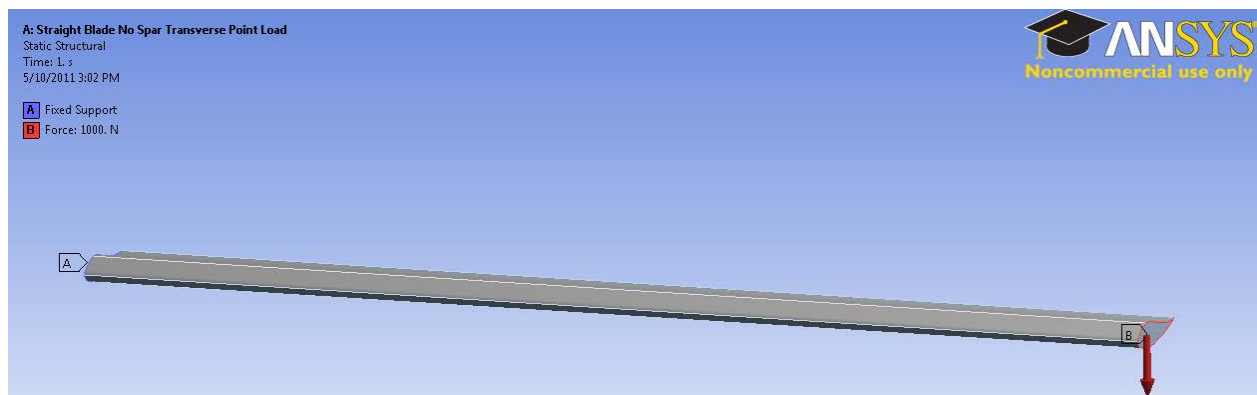


Figure 12: Straight Wing, no Spar Validation Case

We maintained the ANSYS default structural steel material setup, yielding a Young’s Modulus of 200 GPa. We then used ANSYS to solve for the total deformation and the normal stress resulting from our load condition. Figures (13) and (14) show the ANSYS results for deformation and for the normal stress respectively.

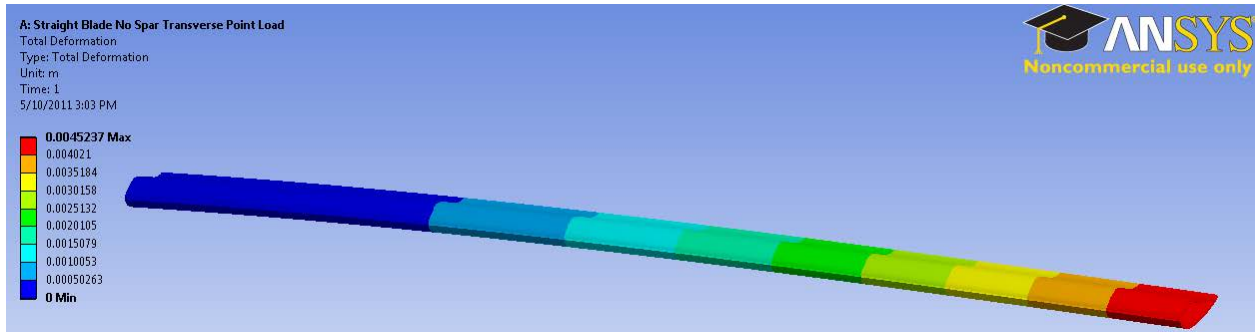


Figure 13: Straight Wing, no Spar Validation Case - Deformation

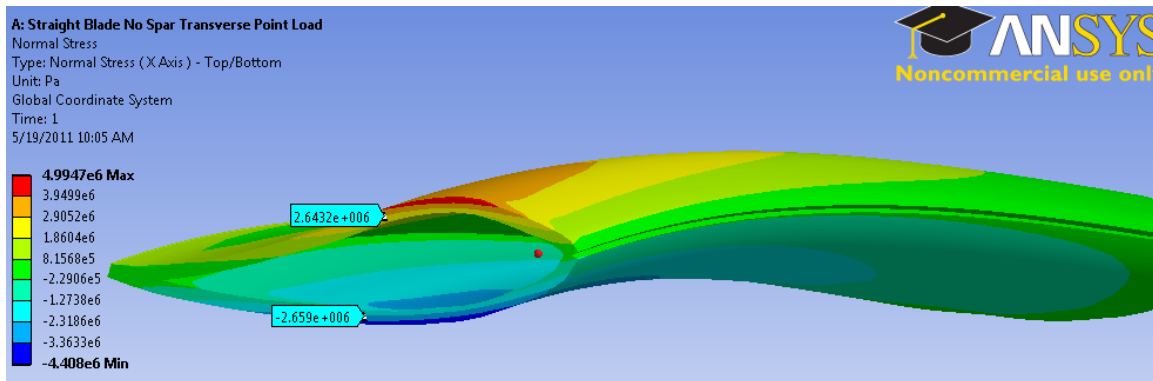


Figure 14: Straight Wing, no Spar Validation Case – Normal Stress

Theoretically, the above problem is a typical beam bending problem. The only component that makes the theoretical computation difficult is the area moment of inertia calculation for the S818 airfoil geometry.

In order to find this moment of inertia we wrote and applied a MATLAB program (see attached MATLAB code “CentMom.m”). The inputs of the program are the x and y coordinates of the desired geometry as well as the thickness of the geometry. The program first computes the centroid location using the following two equations.

$$X_{Centroid} = \frac{\sum_2^{N+1} X_i dS_i}{\sum_2^{N+1} dS_i} \quad (15)$$

$$Y_{Centroid} = \frac{\sum_1^{N+1} Y_i dS_i}{\sum_2^{N+1} dS_i} \quad (16)$$

where the differential arc length, dS is defined

$$dS_i = [(X_i - X_{i-1})^2 + (Y_i - Y_{i-1})^2]^{1/2}. \quad (17)$$

Once the x and y position of the centroid were calculated, the x and y area moment of inertias were calculated using the following two equations:

$$I_x = \sum_1^N h(X_i - X_{Centroid})^2 dS_i \quad (18)$$

$$I_y = \sum_1^N h(Y_i - Y_{Centroid})^2 dS_i \quad (19)$$

where h is the assigned thickness. To ensure the accuracy of this program, we tested the program with simple geometries for which the moments of inertia are known. From there, tip deflection can be found using the following formula:

$$U_{tip} = \frac{PL}{EI} \left(\frac{L^2}{2} - \frac{L^2}{6} \right) \quad (20)$$

where P is the transverse load, L is the length, E is the Young's Modulus and I is the area moment of inertia.

The maximum stress was found using the following formula:

$$\sigma_{max} = \frac{PLc}{I}. \quad (21)$$

The MATLAB program calculated $0.0003719m^4$ for the area moment of inertia. Based on that moment of inertia, the theoretical tip displacement was calculated to be $0.004482m$. The following table displays the theoretical and the ANSYS tip displacement results. Note that the ANSYS results are shown for several different mesh sizes in order to show that the results are mesh converged.

Table 14: Deformation Validation for Straight Wing, no Spar Case

	Tip Displacement (m)
Theoretical	0.00448
ANSYS: 481 elements	0.0048747
ANSYS: 1,088 elements	0.0046592
ANSYS: 2,525 elements	0.0045702
ANSYS: 9,000 elements	0.0045237

Table (15) shows the ANSYS-derived and theoretical results for maximum stress. The highest stress value that ANSYS gives is 4.99 MPa , at the edge of the top of the airfoil, while the stress in the middle of the thickness falls around 2.5 MPa . We believe the 4.99 MPa stress to be an erroneous localized stress concentration that can be neglected.

Table 15: Stress Validation for Straight Wing, no Spar Case

	Maximum Stress (MPa)
Theoretical	2.52
ANSYS	2.64

Straight Blade with Spar Verification

Next, a simulation was carried out for a straight blade with a spar. The geometry consisted of the S818 airfoil extruded to a 10 m length and given a thickness of 0.020 m. The spar was given a thickness of .050 m. The geometry for the setup is shown by Figure (15).

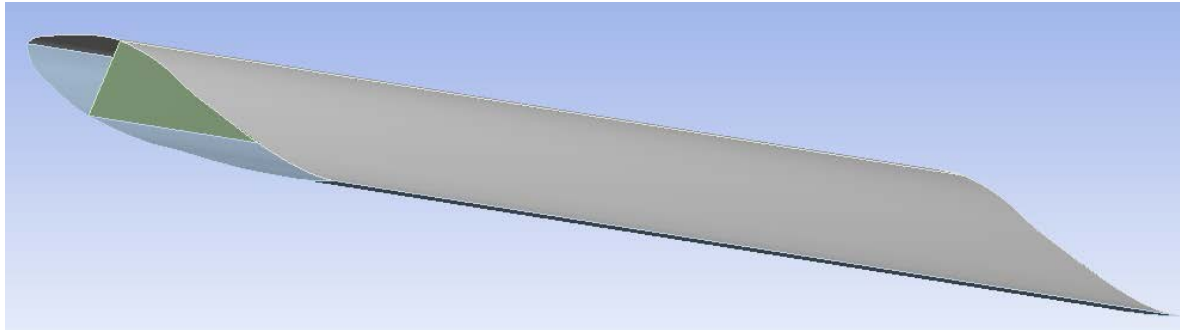


Figure 15: Straight Wing with Spar

Once again, the geometry was assigned a Young's Modulus of 200 GPa. The blade was fixed at one end and assigned a transverse load of 50KN on the other end as shown below.

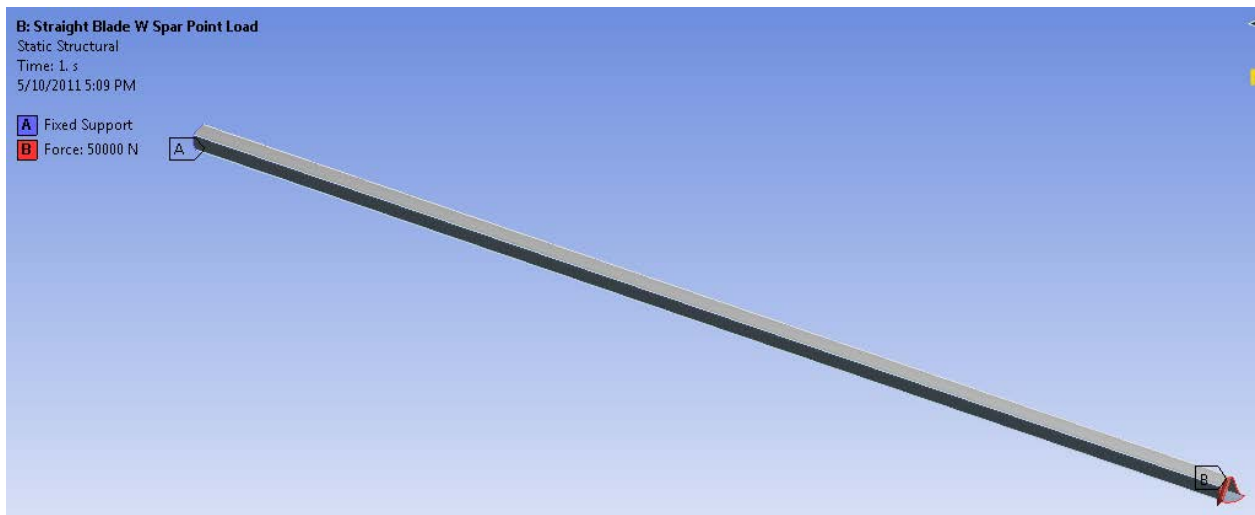


Figure 16: Straight Wing with Spar Loading

The ANSYS simulation yielded the following results for deformation and normal stress respectively.

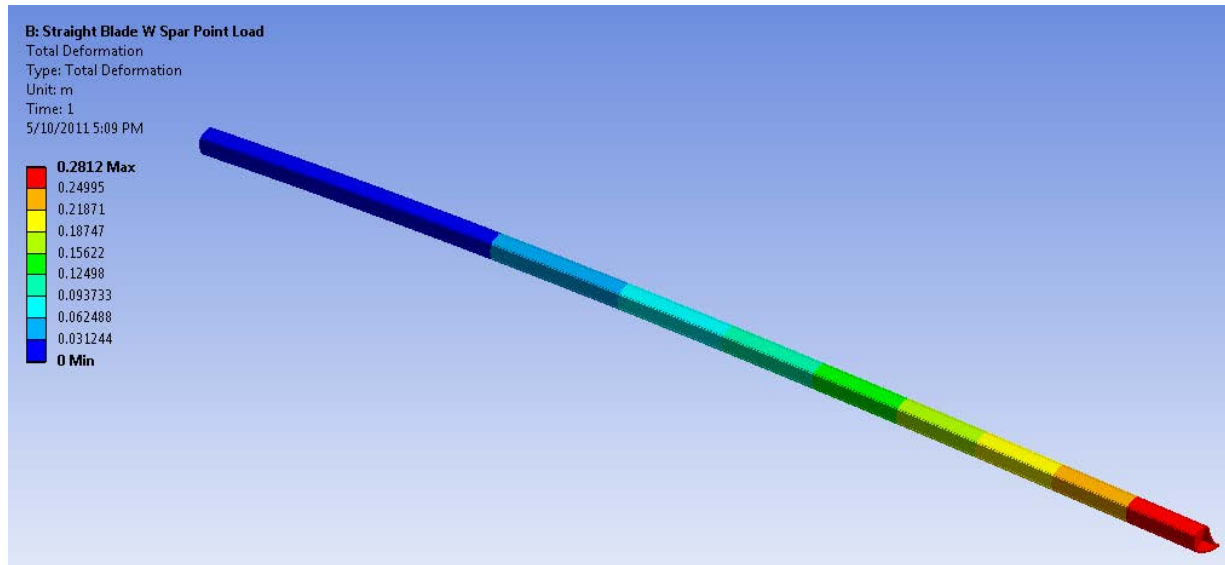


Figure 17: Straight Wing with Spar Validation - Deformation

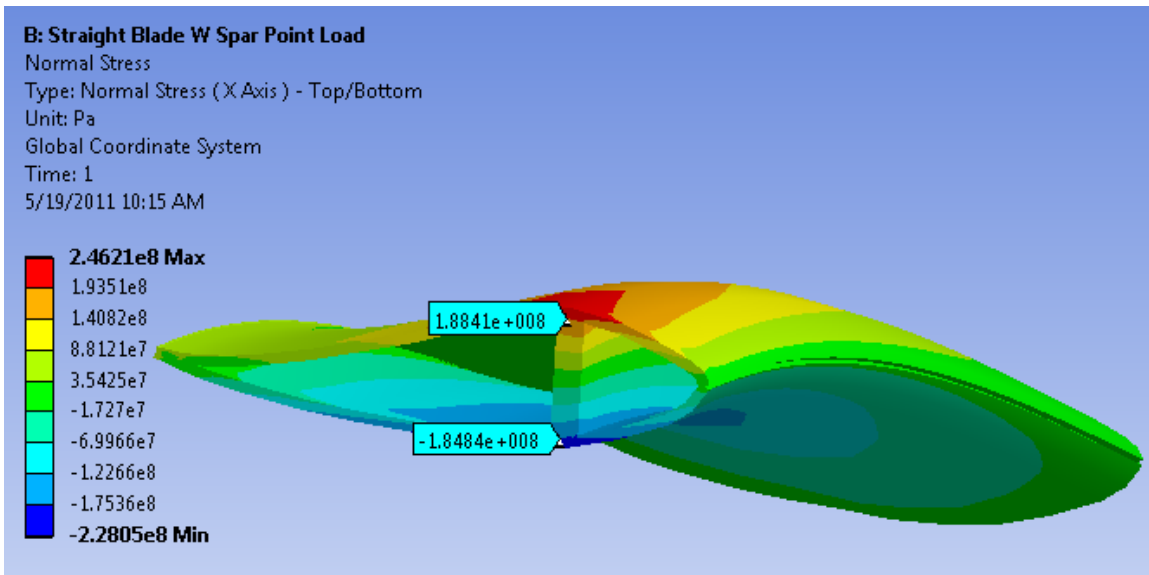


Figure 18: Straight Wing with Spar Validation - Normal Stress

While the area moment of inertia can be calculated in the straight wing case with no spar simply using a numerical summation, it was somewhat more difficult with the inclusion of the spar. The spar has a different thickness than the skin of the wing, and thus shifts the centroid of the airfoil cross-section in a manner not easily captured by the summation of points method described above. Here we instead used a composite cross section method, where the moment of inertia is

$$I_y = \sum (I_{local} + x^2 A) \quad (22)$$

where I_{local} is the moment of inertia for that component (spar or airfoil shape), x the horizontal centroid distance from the y -axis, and A the area of the part. For our purposes, the x and y axes are centered at the centroid of the airfoil shape, so equation (22) simplifies to

$$I_y = I_{airfoil} + I_{spar} + x^2 A_{spar} \quad (23)$$

The airfoil moment of inertia is known from the summation of points described earlier, and the horizontal distance is easily computed since we know the spar to be placed at quarter chord. Likewise, the area of the spar is given simply as base length multiplied by height (.04m and .23m respectively). The area moment of inertia of the spar is given by equation (14). Calculating for these parameter yields a moment of inertia of $2.729 \cdot 10^{-4} \text{ m}^4$ for the wing with spar case.

The table below displays the theoretical and ANSYS results for tip deflection. Once again the ANSYS simulations were ran on different meshes to show mesh convergence.

Table 16: Deformation Validation for Wing with Spar Case

	Tip Deflection (m)
Theoretical	0.307
ANSYS: 1216 elements	0.2864
ANSYS: 2125 elements	0.2824

Table (17) displays the theoretical and ANSYS results for the maximum stress. As one can see from the image above, there is an absolute maximum stress of 246 MPa; however, the stress in the middle of the skin sections is about 188 MPa.

Table 17: Stress Validation for Straight Wing with Spar Case

	Maximum Stress MPa
Theoretical	187.3
ANSYS	184

Full Blade Verification

The purpose of the last verification was to test out the full wind turbine blade geometry. Since the full geometry has varying twist and varying chord length along the blade, the tip deflection cannot be solved for analytically. The maximum stress calculation still holds though.

Furthermore, the area moment of inertia for the maximum stress calculation is quite simple since the root of the blade is a perfect circle. For this simulation the thickness of all parts were set to 20 mm. Once again, the blade was fixed at one end and given a load at the other end. The magnitude of the load was 30kN. ANSYS output the following results for the equivalent von-Mises stresses.

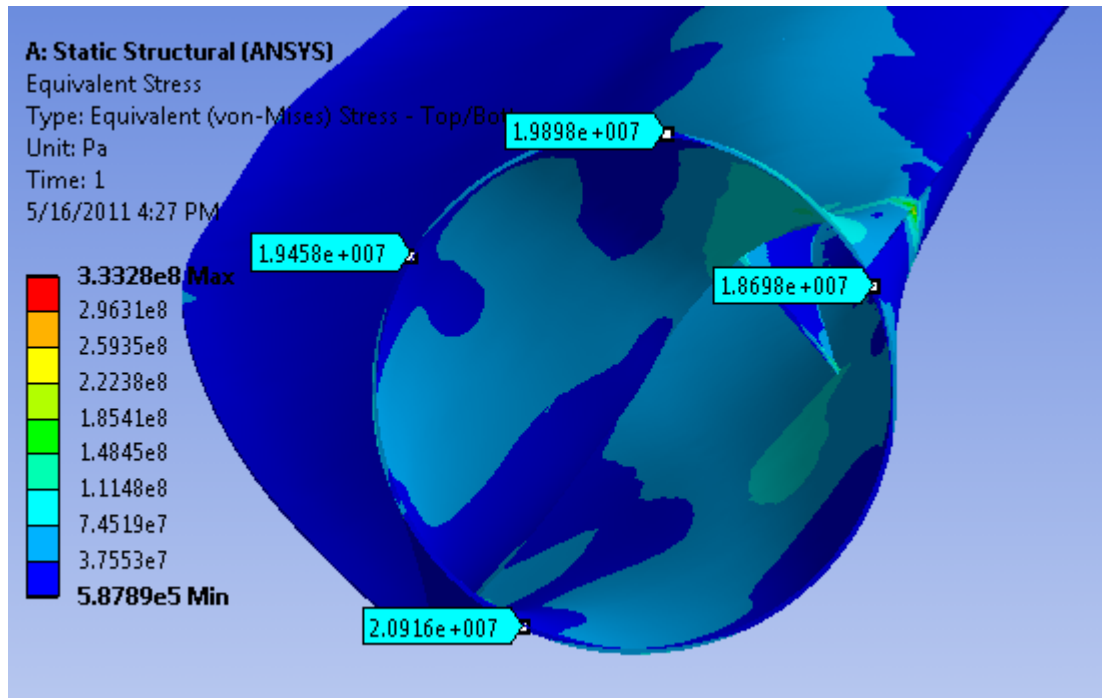


Figure 19: Full Blade Root Stresses

Table (18) shows how the ANSYS results compare to theoretical results. As can be seen from the image above, there is an absolute maximum stress of 333 MPa in the model (this occurs at the origination point of the spar); however, the stress in many areas around the root section is around 20 MPa.

Table 18: Root Stress Validation for Full Blade

	Maximum Stress MPa
Theoretical	19.6
ANSYS	20

Full Blade ANSYS Implementation:

This section will serve to describe how the full blade simulation was created in ANSYS. Many difficulties were encountered during the process, so the solutions will be outlined here.

Geometry

The geometry for the wind turbine blade was created within SolidWorks. As we wished to work with ANSYS shell elements for computational efficiency, the SolidWorks model (consisting of 3 parts – top half of airfoil, bottom half of airfoil, and spar) was created using surface lofts. The completed SolidWorks blade was then imported into the ANSYS Design Modeler as a “frozen”. It was important to import the geometry as a “frozen”, as this allowed the geometry to be partitioned.

We partitioned the model so that we could apply different loads at different sections of the blade. It was decided to partition the blade into 5 equal spanwise segments. The length of the full blade is 41.25 m, so the length of each of the five segments was 8.25m. In order to partition the blade, a special extrusion feature was used. For instance, imagine that the span of the blade falls on the x axis, with the root at the origin. In order to make the first division, a rectangle was

drawn on the YZ plane that could encompass the cross section of the blade. Next, the rectangle was extruded to 8.25 m, except the “operation” of the extrusion was set to “slice material”. In order to make the next division, a plane parallel to the YZ plane was created at $x=8.25\text{m}$. Then a rectangle was drawn on this plane and extruded with the “slice material” operation. This procedure was then repeated two more times in order to create the five partitions. Figure (20) shows the geometry of the model after partitioning.

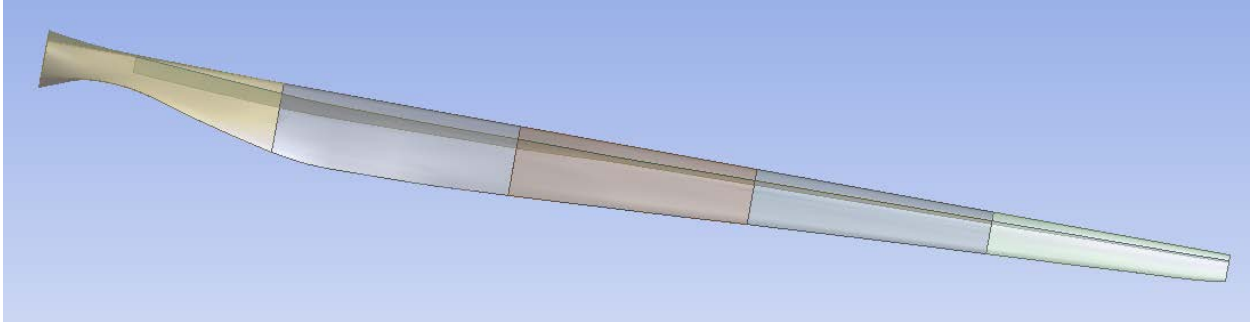


Figure 20: Full Blade Partitioned into Sections

After the geometry was partitioned the parts had to then be put together. For each spanwise partition there are three pieces: a top airfoil half, bottom airfoil half and spar. Thus, there were 15 pieces in total. In order to form one cohesive part out of the 15 pieces, you highlight all of the pieces in the tree outline, right click, and select “Form New Part”. The formation of the single part is a very important step; if it is not taken the simulation will not work.

Meshing

Prior to discussing the meshing, it must be mentioned that ANSYS creates false “Connections” when importing the geometry into the Mechanical editor. There should be no “Connections” as all the 15 pieces should be the constituents of one cohesive part. Thus, the faulty “Connections” were simply deleted. In order to delete the faulty “Connections”, the “Connections” label in the tree outline was expanded and all of the “Connections” within were deleted. Next, mesh sizing commands were given to each of the five partitions. For each partition a “Body Sizing” command was implemented. The three parts of each partition (bottom half, top half and spar) were applied as the geometry of the “Body Sizing” command. Once, the five “Body Sizing” commands were implemented the resolution of the mesh could be manipulated with ease. The following picture shows a coarse mesh in which the element size for all five “Body Sizing” commands was set to 0.6m.

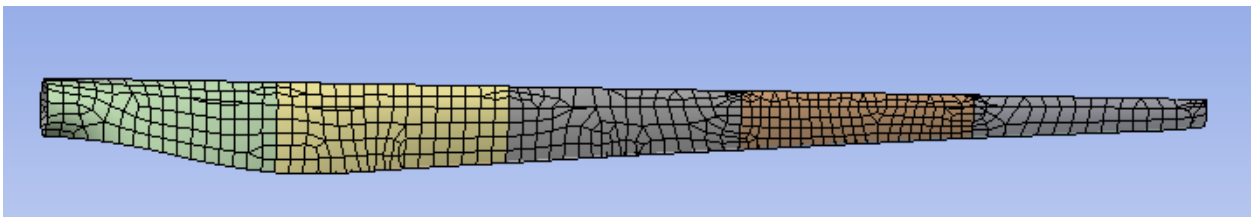


Figure 21: Full Blade with Coarse Mesh

The advantage of having “Body Sizing” commands for each section is that one section can be given higher resolution. For instance, in Figure (22) the element size for the root section was set to 0.3m, whereas the element size for the four other “Body Sizing” commands were set to 0.4m.

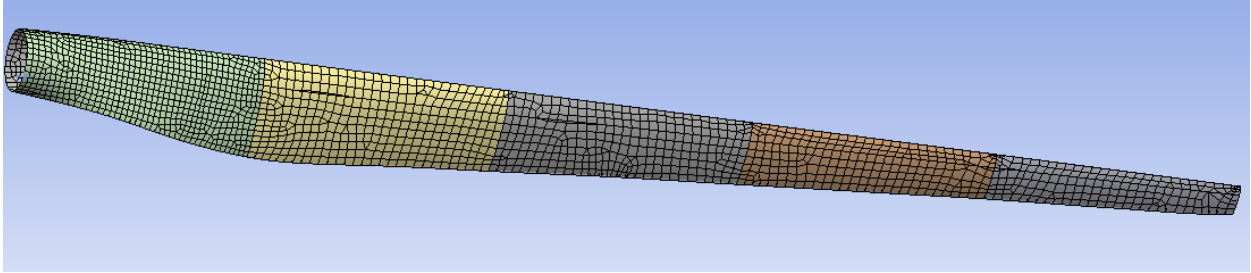


Figure 22: Full Blade Final Mesh

It can be seen that there are significantly more elements in the root section than the other four sections, which is useful due to the complicated geometry of the root transition from circular hub to S818 airfoil. This was the mesh used for the final simulations.

Material Properties and Thickness

ANSYS does not have a feature in its GUI that allows varying of shell thickness as a function of position. In order to incorporate varying thicknesses we used command “Snippets”. For each of the fifteen pieces of the wing geometry a command “Snippet” was needed. These command “Snippets” specified the material properties as well as thickness for that particular piece. ANSYS defines equations in three dimensional matrices. Thus, in order to specify a thickness one must first create the three dimensional matrix that defines the desired thickness equation. In order to create the equation matrix, the older form of ANSYS, Mechanical APDL, was used. The equation matrices were found by defining functions within the “Function Tool” in APDL and saving the file. The saved files were then opened with a text editor where the three dimensional matrices can be found. The matrices were then copied into the command “Snippets” in order to define the thickness function. It must also be mentioned that one additional command “Snippet” was placed in the analysis portion of the simulation. This last command “Snippet” essentially forbids ANSYS from overriding anything that was specified in the previous command “Snippets”. For an example of a “Snippet” that specifies thickness and material properties as well as the analysis section “Snippet”, see the attached code within Appendix B.

Loading

For the simulation, the root section of the blade was fixed using the “Fixed Support” command. In order to apply the loads to the blade a “Force” command was created for each of the five partitions. The “Force” commands were applied to the top and bottom half of the blade for each section. The forces on each blade section were then defined in component form (the F_z and F_y values obtained using WT_Perf).

Optimization

We wished to iterate our blade design to obtain a blade that incorporated as little material as possible while still meeting key design criteria. The basic premise was to apply the loading for the cut-out speed of 20 m/s to the blade and adjust the thickness of each of the three parts such that these design constraints were satisfied.

The first design limit ensures that the blade could not hit the turbine tower. It was estimated that the blade was 4 m away from the tower at the hub. Turbine blades, however, are generally inclined such that the blade is angled away from the tower when pointing towards the ground. Using a blade inclination of 5 degrees, we determined that the deflection of the blade tip could not exceed 7.6 meters.

The second design constraint was that the stress in the spar could not exceed 1200 MPa, the fatigue limit of P2B carbon laminate. The final design limit was that the stress cannot exceed 120 MPa, the fatigue limit of QQ1 E-glass, in the skin of the blade. The design of the blade and its iterations focused primarily on the deflection and skin stress design limits, as the stress within the carbon fiber spar never approached its limit.

The root section of the blade was fixed and the five sections were given the following loading, which is based on the WT_Perf data for the 20 m/s wind speed case.

Table 19: Full Blade Section Forces - Cut-out Wind Speed

Section	F _y (N)	F _z (N)
1	5868	345
2	14763	447
3	23445	2828
4	33908	7184
5	39321	8791

The spar was given a Young's Modulus of 101 GPa and the blade halves were given a Young's Modulus of 33 GPa. First we varied the spar thickness to determine what was needed to limit the total deformation to fall below 7.6m. Next, the skin thickness functions were varied to ensure the stress remained below 120MPa. The optimal configuration turned out to be a constant spar thickness of 10 cm and a linearly varying thickness for the blade. The optimal thickness equation for the blades was a linear function with 30 mm thickness at the root and 10 mm thickness at the tip. The aforementioned thicknesses and loading yielded the following deformation and normal stress respectively.

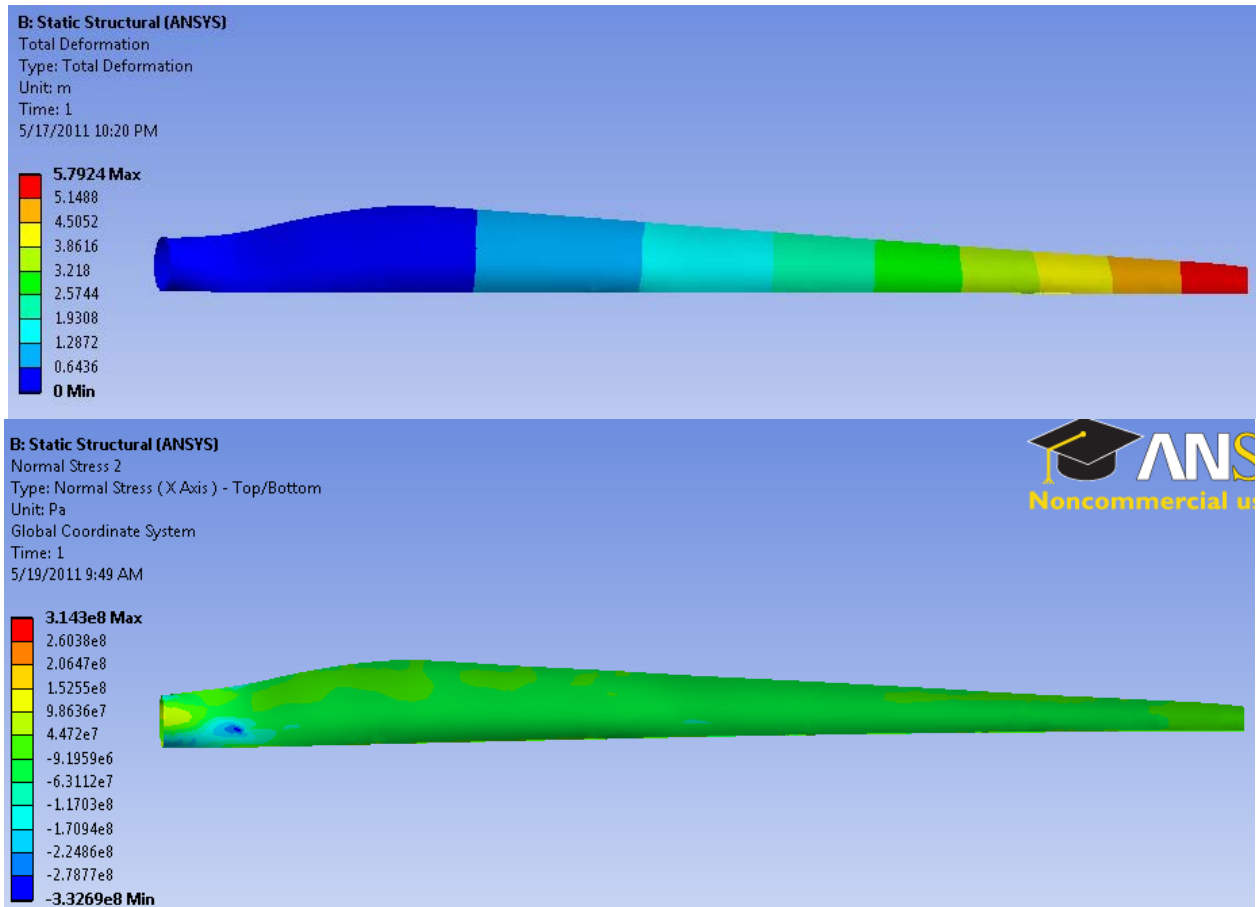


Figure 23: Full Blade Deformation and Stress for Cut-Out Wind Speed

It can be seen that ANSYS calculates a stress concentration approximately 3m from the blade root. This concentration is due to the contact between the beginning of the spar and blade and can be neglected. Aside from this small stress concentration where the spar begins, the stresses within the blade fall well below the design criterion. The deformation also falls well below the design limit with a value of 5.79m.

After optimized thicknesses were found we re-ran the simulations run for the rated case of 10 m/s wind. The loading for this case (based on WT_Perf) is shown by Table (20).

Table 20: Full Blade Section Loads - Rated Wind Speed

Section	F _y (N)	F _z (N)
1	4923	436
2	13723	1715
3	22725	1981
4	30324	2516
5	24521	1766

These loading conditions yielded the following results in ANSYS for deformation and normal stress respectively.

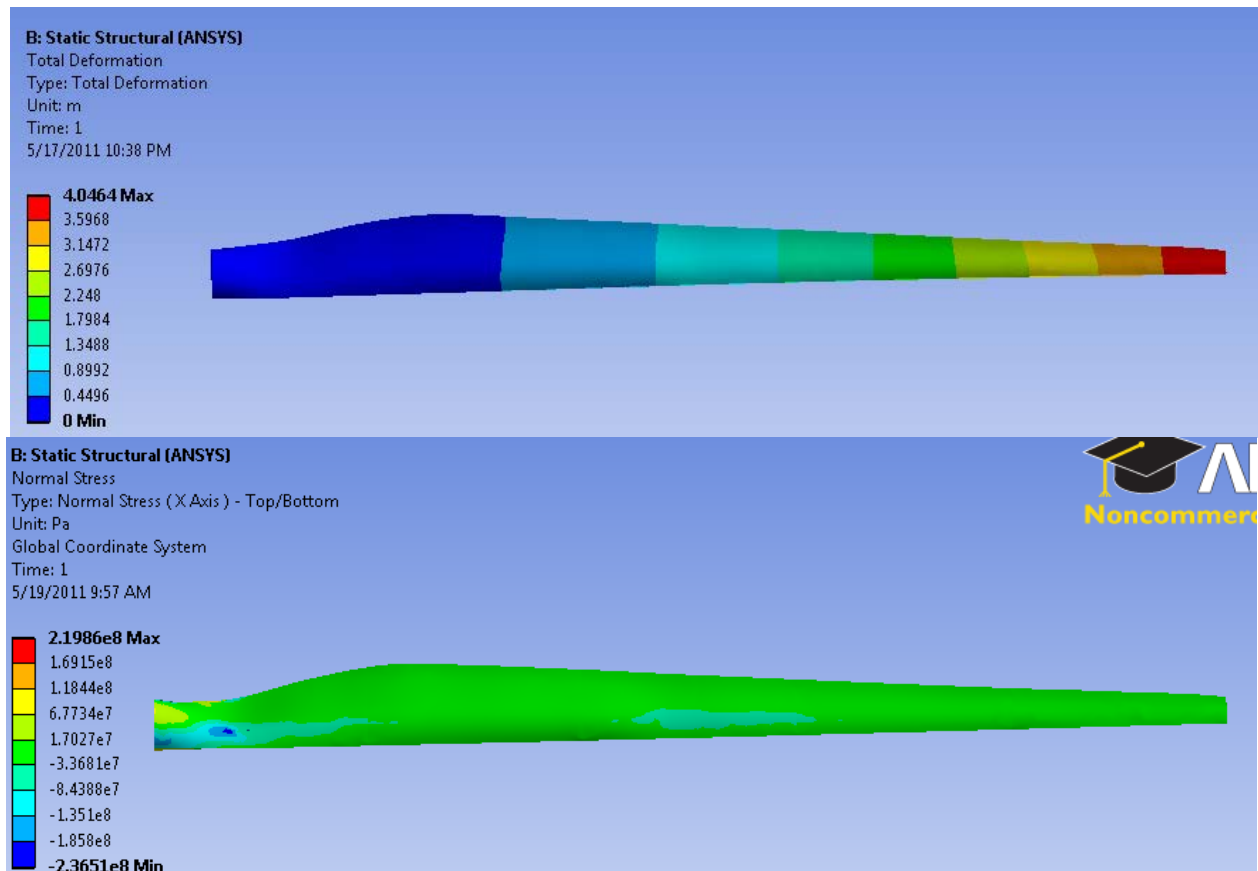


Figure 24: Full Blade Deformation and Normal Stress for Rated Wind Speed

Once again the small stress concentration appears at the start of the spar, and once again we neglect this inflated stress value. Throughout the remainder of the blade the stress is far below the maximum skin stress, and the deformation within its limits.

Thus, the optimal spar thickness for our blade is a constant 10 cm and the optimal skin thickness is a linearly varying function with a root thickness of 30mm and a tip thickness of 10mm.

Comparisons and Results

After deciding upon the blade geometry and material properties, it was of interest to compute a first pass estimate of the material cost for the blade. In order to calculate this value, we first determined the total mass of used of each blade component. The mass of spar was found to be 3030 kg and the total mass of the skins was found to be 9940 kg. Assuming that the carbon laminate can be purchased for \$11/kg and that QQ1 E-glass can be purchased for \$2/kg, the cost of the blade materials would be \$53,210.

We were able to effectively model our blade and optimize it to minimize material use while maximizing material and design specifications. Also of interest, however, was how this computational result compared with those values obtained from our analytical solutions.

As shown in Table (6), when we use the flapwise bending moment obtained from the equation (1) analytic solution for M_β , the blade thickness should be 31.5mm. The moment used here, however, is an estimation based on the maximum value for the axial induction factor. Accordingly, this solution results in what should be an overbuilt blade root. Using the flapwise bending moment obtained from WT_Perf ($M_\beta = 2.875$ MN-m) and equation (7), we find that the necessary thickness should be 7.71mm.

However, it is important to note that, again, WT_Perf load are all done in local coordinates. The flapwise moment calculated is thus not necessarily what was input into ANSYS. The flapwise moment using the ANSYS global coordinate system can be determined through statics, using the F_y values from Table (10) and the average span distance from the section in question. The total flapwise moment is merely a summation of these induced section moments, and equals 3.361 MN-m. Using the thickness equation (7), the necessary root thickness would then be 9.04mm. A comparison of the various moments can be seen below:

Table 21: Necessary Root Thicknesses for Various Conditions (at cut-out wind speed, fatigue incorporated)

	M_β (MN-m)	Thickness (mm)
Moment derived analytically from Betz limit	11.31	31.5
Moment given in WT_Perf	2.875	7.71
Moment from ANSYS loads	3.361	9.04
ANSYS Model	3.361	30.0
Extreme winds (70 m/s) with 0° pitch	7.386	20.2

Table (21) shows the flapwise bending moments and the necessary thicknesses they incur from the analytic solution for thickness (the exception being the ANSYS model thickness, which was optimized within the program for that root thickness). It is interesting to note that the calculated thickness closest to what is actually required comes from the analytic solution where the moment was derived from the Betz limit axial induction factor. All other analytic solutions underestimate the necessary skin thickness at the root. Though the Betz limit derived moment yields a value close to what we actually determined from our computations, the similarity seems serendipitous given the significant difference in the flapwise moment. Given the data, it seems likely that our first pass analytic solution for thickness generally underestimates the necessary thickness needed at the root. The extreme winds case, for instance, still yields a necessary thickness less than the Betz limit derived moment case or ANSYS given thickness.

In addition to the flapwise bending moment, however, we also wished to compare the edgewise bending moments calculated with what we obtained from our FEA analysis. The edgewise moment can be calculated analytically using equation (3). It is worth noting that the value here changed slightly from our first pass solution, as the weight term was solved for as opposed to simply assuming the blade to be 10 metric tons.

After the optimal blade configuration we were able to calculate the mass of the blade. The blade is made out of QQ1-E-glass and P2B carbon laminate with densities of 2.53g/cm^3 and 1.78g/cm^3 , respectively. We defined these densities within ANSYS, and applied them to the appropriate sections of the blade. We then defined a skin thickness of 20mm and a spar thickness of 100mm. This approximation of skin thickness (which varies along length) had to be done, as ANSYS will not read thickness values from command “Snippets” for mass calculation. 20mm was chosen as it is the average thickness of the skin (which varies from 30mm to 10mm along the span of the blade). With material densities and thicknesses applied, ANSYS reported a total blade mass of 12,969 kg. This yields a weight of 127.2 kN, and the maximum edgewise moment is therefore 2.07 MN-m. The edgewise moment input into the ANSYS model can be calculated similarly to the flapwise moment, performing a summation of F_E multiplied by moment arm for each section. The comparison of edgewise moments can be seen in Table (22).

Table 22: Edgewise Bending Moment Comparison

	M_E (MN-m)
Analytic Solution	2.07
ANSYS Model	.637

In the analytic solution, it is worth noting that now the edgewise bending moment has increased from our first-pass solution due to the increased weight of the blade. The moment calculated is still small compared to the Betz limit derived flapwise moment, but is relatively high compared to the WT_Perf and ANSYS model flapwise moments. Even assuming those smaller values for M_β , however, the flapwise moments remain the main drivers for structure. The ANSYS model edgewise moment is notably small, which is likely due to the absence of weight as a factor. In the analytic solution for instance, the weight driven moment term actually accounted for around 86% of the moment. So while the weight from a large turbine may not be a driving design factor from a structural standpoint, it is nonetheless the driving factor in the value of the edgewise moment.

Future Work

While we were able to compute some effective design parameters for the blade, and managed to optimize across a several design parameters, there is nonetheless much that could be done to improve our analysis.

The first parameter that could likely have a large impact on the blade design would be to vary the thickness of the spar along the length of the blade. The P2B carbon laminate spar is currently a 10cm block of carbon that runs the entire length of the blade (excepting the region near the root). It is likely that the spar need not be that built up along the entire length of the blade, and practically speaking it could result in significant cost savings if the amount of that material were able to be reduced. These changes would of course be made keeping the deflection and carbon stress design limits in mind.

Additionally, it would be helpful to analyze the structural performance of the blade with other pitch angles taken into account. Here we decided to stick with 0° of deflection for our rated and cut-out cases in order to perform more in-depth analysis on them, but it would be interesting to

note how varying those pitch angles might influence our blade design, if at all. While we were able to determine extreme load flapwise moments with both significant pitch (which is desirable) and no pitch (liable to damage the blade), similar analysis at other wind speeds would be useful.

Another factor that might play a great role in improving our blade design and ensuring enhanced validity of the model would be to incorporate proper composite lay-up properties into the model. The material properties we used for both the QQ1 E-glass and carbon laminate were valid properties and defined by particular lay-ups, but we simplified our model by simply assuming these materials to be isotropic. They are, of course, not isotropic, and it would be very interesting to see how incorporating this dynamic into our material properties might change our design characteristics.

In short, our work this year, though useful and productive, nonetheless has multiple layers of additional complexity that could be added to improve our model. Inclusion of additional internal geometries like spar caps, analyses at additional pitch angles, inclusion of more precise material constraints; all these factors and more can be added to make our model better and to better design around the appropriate figures of merit.

Appendix A: Centroid and Moment of Inertia Calculation

CentMom.m

```
%*****  
% 'CentMom' written by John M. Singleton on 04/30/2011  
% This program finds the centroid position and the moment of inertia for  
% the geometry that the user provides. User must supply a txt file with  
% coordinate data (one column array of x position and one column array of  
% y position). User must also define the shell thickness which is defined  
% as a middle offset.  
%*****  
  
clc % Clear Command Window  
close all % Close Any Open Figures  
clear all % Clear Variable Space  
  
%Create an Ellipse with a=2 and b=1 For Testing Purposes  
% Actual Moment:  $I_x=(1/4)*\pi*a*b^3$  &  $I_y=(1/4)*\pi*a^3*b$  For filled Ellipses  
x_ellipse=2*cos(thet);  
y_ellipse=sin(thet);  
pos=[x_ellipse; y_ellipse];  
fid = fopen('ellipse.txt','w');  
fprintf(fid,'%4f %4f\n', pos);  
fclose(fid);  
  
h=.020; %Define The Shell Thickness [m] **User Defined**  
data=load('circle.txt'); % Load the Point Data **User Defined**  
  
NumbCoord=size(data,1); % Determine the Number of Coordinate Points  
  
for j=1:NumbCoord %Centroid Loop  
    if (j==NumbCoord)  
        ds(j)=sqrt(((data(j,1)-data(1,1))^2)+((data(j,2)-data(1,2))^2));  
    else  
        ds(j)=sqrt(((data(j,1)-data(j+1,1))^2)+((data(j,2)-data(j+1,2))^2));  
    end  
    xds(j)=ds(j)*data(j,1);  
    yds(j)=ds(j)*data(j,2);  
end  
  
S=sum(ds);  
CentX=sum(xds)/S; %Compute The X Centroid Location  
CentY=sum(yds)/S; %Compute the Y Centroid Location  
  
for i=1:NumbCoord %Moment of Inertial Loop  
    if (i==NumbCoord)  
        ds(i)=sqrt(((data(i,1)-data(1,1))^2)+((data(i,2)-data(1,2))^2));  
    else  
        ds(i)=sqrt(((data(i,1)-data(i+1,1))^2)+((data(i,2)-data(i+1,2))^2));  
    end  
end
```



```
ds(i)=sqrt(((data(i,1)-data(i+1,1))^2)+((data(i,2)-data(i+1,2))^2));
end
dl_x(i)=h*ds(i)*(data(i,1)-CentX)^2;
dl_y(i)=h*ds(i)*(data(i,2)-CentY)^2;
end

I_x=sum(dl_x); %Compute The X Moment of Inertia
I_y=sum(dl_y); %Compute The Y Moment of Inertia

%Output The Results
fprintf('The X Centroid Position is %.10f\n',CentX)
fprintf('The Y Centroid Position is %.10f\n',CentY)
fprintf('The X Moment of Inertia is %.10f \n',I_x)
fprintf('The Y Moment of Inertia is %.10f \n',I_y)

% Plot The Geometry
figure(1)
plot(data(:,1),data(:,2),'b-*',CentX,CentY,'r*')
```

Appendix B: Thickness & Material Properties ANSYS "Snippet"

Thickness and Mat Prop "Snippet"

```
/prep7          !Call the Preprocessor

et,matid,181    !Specify the element type, shell 181
keyopt,matid,3,2 !Use full integration
mpdel,all,matid !Delete all previously assigned material properties
tbdel,all,matid !Delete all previously assigned tabular data

MP,EX,1,33E9   !Define Young's Modulus: X Direction
MP,EY,1,33E9   !Define Young's Modulus: Y Direction
MP,EZ,1,33E9   !Define Young's Modulus: Z Direction

MP,PRXY,1,0.3  !Define Major Poisson's ratio XY
MP,PRYZ,1,0.3  !Define Major Poisson's ratio YZ
MP,PRXZ,1,0.3  !Define Major Poisson's ratio XZ

*DIM,vth,TABLE,6,5,1 !Dimension The Table for the Thickness Function

! Begin of equation: .025-{X}*.00036364
!25mm at root, 10 mm at tip
vth(0,0,1)= 0.0, -999
vth(2,0,1)= 0.0
vth(3,0,1)= 0.0
vth(4,0,1)= 0.0
vth(5,0,1)= 0.0
vth(6,0,1)= 0.0
vth(0,1,1)= 1.0, -1, 0, .00036364, 0, 0, 2
vth(0,2,1)= 0.0, -2, 0, 1, 2, 3, -1
vth(0,3,1)= 0, -1, 0, .025, 0, 0, -2
vth(0,4,1)= 0.0, -3, 0, 1, -1, 2, -2
vth(0,5,1)= 0.0, 99, 0, 1, -3, 0, 0
! End of equation: .025-{X}*.00036364
!-->

sect,1,shell    !Specify the section type
secfunction,%vth% !Apply the Varying Thickness Function
```

Analysis Section "Snippet"

```
fini          !Exit current Module
/prep7        !Call the preprocessor
etcon,off     !Disable ANSYS from changing any KEYOPTS
fini          !Exit the preprocessor
/solu         !Call the Solve Module
```

Works Cited

ANSYS. (n.d.). Mechanical APDL Verification Manual.

Beer, F. P., Johnston, E. R., & DeWolf, J. T. (2006). *Mechanics of Materials* (4th Edition ed.). New York, NY: McGraw-Hill.

Grande, J. A. (n.d.). *Wind Power Blades Energize Composites Manufacturing*. Retrieved December 12, 2010, from PlasticsTechnology:
<http://www.ptonline.com/articles/200810fa2.html>

Lawrence, K. L. (2010). *ANSYS Workbench Tutorial*. Schroff Development Corporation.

Manwell, J. F., McGowan, J. G., & Rogers, A. L. (2002). *Wind Energy Explained: Theory, Design and Application*. Chichester, NY: Wiley.

Materials Database. (n.d.). Retrieved December 1, 2010, from Matbase:
<http://www.matbase.com/material/fibres/glass/e-glass-fibre/properties>

Nolet, S. C. (2010, March 10). *Manufacturing of Utility-Scale Wind Turbine Blades*. Retrieved December 12, 2010, from Iowa Wind: <http://www.iawind.org/presentations/nolet.pdf>

Samborsky, D. D., Wilson, T. J., & Mandell, J. F. (2007). Comparison of Tensile Fatigue Resistance and Constant. *AIAA* .

Stress in Thick-Walled Tubes or Cylinders. (n.d.). Retrieved October 19, 2010, from The Engineering ToolBox: http://www.engineeringtoolbox.com/stress-thick-walled-tube-d_949.html

The Windpower. (2010). Retrieved November 16, 2010, from
<http://www.thewindpower.net/fiche-eolienne-technique-58-ge-energy-1.5xle.php>

TPI Composites, Inc. (2002). *Parametric Study for Large Wind Turbine Blades*. Warren, RI: Sandia National Laboratory.

Composite / Steel Cost Comparison. MIT Materials Systems Laboratory. Retrieved 05/19/2011 http://msl1.mit.edu/MIB/3.57/LectNotes/gm_tech_composites.pdf